A feeder protection method against the phase-phase fault using symmetrical components

Ciontea, Catalin-Iosif; Bak, Claus Leth; Blaabjerg, Frede; Madsen, Kjeld Kilsgaard; Sterregaard, Claes Høll

Published in:
Proceedings of the 2017 IEEE Electric Ship Technologies Symposium (ESTS)

DOI (link to publication from Publisher):
10.1109/ESTS.2017.8069260

Publication date:
2017

Document Version
Accepted author manuscript, peer reviewed version

A feeder protection method against the phase-phase fault using symmetrical components

Catalin Iosif Ciontea, Claus Leth Bak,
Frede Blaabjerg
Department of Energy Technology
Aalborg University
Aalborg, Denmark

Catalin Iosif Ciontea, Kjeld Kilsgaard Madsen,
Claes Høll Sterregaard
Department of Research and Development
DEIF A/S
Skive, Denmark

***Abstract*—the method of symmetrical components simplifies analysis of an electric circuit during the fault and represents an important tool for the protection engineers. In this paper, the symmetrical components of the fault current are used in a new feeder protection method for the maritime applications. The new method is effective against the phase-phase fault and relies on evaluation of the ratio of negative-sequence to positive-sequence current to detect such faults. It is shown that the proposed ratio is a complex number and its magnitude is associated with the presence of the phase-phase fault in a radial feeder, while its argument is an indicator of the fault direction. Precisely these information are used in this paper to detect the phase-phase fault and to indicate the faulted section of the feeder. Using PSCAD, the new method is implemented in a test Medium Voltage feeder with variable generation and relatively reduced short-circuit currents, thus resembling the electric network on a ship. The simulation results demonstrate that the proposed method of protection provides an improved performance compared to the conventional OverCurrent relays in a radial feeder with variable short-circuit power.**

Keywords—symmetrical components, phase to phase fault, radial feeder, variable short-circuit currents, maritime sector

I. INTRODUCTION

The electric network is an important part of any ship as it provides power to the essential systems, including propulsion, navigation, signaling and other critical equipment [1]. Both DC and AC (at 50 Hz or 60 Hz) power systems are used in the maritime sector [2], [3], but the focus of this paper is on the AC networks at Medium Voltage (MV) level. Such networks can be regarded as radial power system with different degrees of redundancy such that a single defect within its structure does not cause the loss of the essential systems [2], [3]. Generation is realized using several generators and is variable, as loading of the ship is variable as well [1]. The three-phase loads are typically balanced and are connected on several bus bars that are interconnected by distribution feeders and tie-breakers.

Protection against the electric fault is of utmost importance for proper operation of a ship and for personnel safety [1]. Due to the specific nature of the maritime networks, protection against the electric fault represents an interesting topic and sometimes a challenging one as well. For example, variable generation implies that the available short-circuit power is also variable, thus causing coordination problems or longer tripping times for the OverCurrent (OC) relays [4]. Consequently, the conventional OC protection needs a revision in the maritime applications that are characterized by a high level of variability of the fault current.

The method of symmetrical components is used in [5] for analysis of various fault conditions in a maritime network. The results suggest that the conventional OC protection could be improved in some situations by utilization of the sequence components of the fault current. As a continuation of the work presented in [5], this paper proposes a new feeder protection algorithm that uses the same quantities as in [5] for detection of the Phase-Phase (PP) fault. However, instead of using directly the magnitude of the negative-sequence current as an indicator of the PP fault, this paper proposes utilization of the ratio between the negative-sequence and positive-sequence current to detects the PP fault. The proposed protection method uses communication between the adjacent relays to coordinate their operation and to detect the faulted section of the feeder.

The major advantage of the new protection method over the conventional OC protection in a radial feeder is that it provides adequate protection when the available short-circuit power is variable. More precisely, the new method is less sensitive to the variable or reduced short-circuit power and does not require a prior knowledge of the rated currents and fault currents in the protected network. Also, it needs to be mentioned that the communication infrastructure might be already available in a ship for control purposes [4], thus facilitating implementation of the proposed protection scheme in such applications. The setting procedure of the relays that use the proposed protection algorithm is relatively simple in a radial feeder and a single set of settings is valid for a wide range of network conditions.

The remaining of this paper is structured as follows. In Section II and Section III, the theoretical background of the proposed method of protection is discussed. In Section II, the PP fault is analyzed in a simple circuit using the method of symmetrical components, while in Section III the PP fault is analyzed in a simple radial feeder. Based on these analysis, the new method of protection is described. Investigation of the proposed algorithm is realized using PSCAD in a test maritime MV feeder for various system conditions. The modeling of the test MV feeder is described in Section IV, while the simulation results are presented and discussed in Section V. Finally, the paper ends with some final remarks and conclusions.

II. PROPOSED METHOD

A. Symmetrical components

Symmetrical components of a three-phase current can be calculated using the mathematical transformation given in (1).

$$\begin{bmatrix} I_0 \\ I_1 \\ I_2 \end{bmatrix} = \frac{1}{3} \cdot \begin{bmatrix} 1 & 1 & 1 \\ 1 & a & a^2 \\ 1 & a^2 & a \end{bmatrix} \cdot \begin{bmatrix} I_a \\ I_b \\ I_c \end{bmatrix} \quad (1)$$

I_a, I_b, I_c are the phase currents, I_0, I_1, I_2 are the zero, the positive, respectively the negative-sequence components of the three-phase current referred to the phase a [6], while a is the phasor rotation operator given in (2).

$$a = 1\angle 120° = -\frac{1}{2} + j \cdot \frac{\sqrt{3}}{2} \quad (2)$$

The positive-sequence components of a three-phase current are always present in a power system, while the other sequence components appear in unbalance or fault conditions [6]. For example, during the PP fault the negative-sequence currents are generated at the fault location and propagate throughout the network [6]. These quantities can be detected by the protection relays and used for protection purposes against the PP fault, as indicated in the following sections.

B. Analysis of the Phase-Phase fault

Fig. 1 illustrates a simplified electric network used for analysis of the PP fault. It consists of a balanced delta load supplied by a star-connected power source whose star point is earthed through a resistance R_G. E, a^2E and aE represent the internal e.m.f. of the power source on each phase, where a is the rotation operator given in (2). The equivalent impedances of the source and of the load are denoted Z_S, respectively Z_L. A set of 3 Current Transformers (CTs) is used for monitoring of the supplied currents, denoted I_{a_CT}, I_{b_CT}, respectively I_{c_CT} and a PP fault with the fault resistance R_F is considered as shown in the figure. During the PP fault, the source continues to supply the load, therefore each of the currents measured by the indicated CTs is composed of 2 components: the fault current and the load current. In Fig. 1, the following notations are used: I_{a_F}, I_{b_F} and I_{c_F} represent the fault currents, while I_{a_L}, I_{b_L}, and I_{c_L} are the load currents.

Analysis of the described network seeks to determine the positive and negative-sequence components of the previously introduced currents for the considered PP fault. The equivalent sequence diagram of the simplified electric network in PP fault conditions is illustrated in Fig. 2, where the following notations are used for the sequence impedances: Z_{0_S}, Z_{1_S}, Z_{2_S} and Z_{0_L}, Z_{1_L}, Z_{2_L} represent the zero, positive and negative-sequence impedances of the source and of the load respectively. I_{1_CT}, I_{2_CT} and I_{0_CT} are symmetrical components of the currents seen by the CTs, I_{1_F}, I_{2_F} and I_{0_F} are symmetrical components of the fault currents, while I_{1_L}, I_{2_L} and I_{0_L} represent symmetrical components of the load currents during the fault.

I_{1_CT} is obtained after resolution of the sequence diagram shown in Fig. 2 and it is given in (3), where Z_2 represents the equivalent negative-sequence impedance and it is given in (4).

$$I_{1\_CT} = \frac{E}{Z_{1\_S} + Z_{1\_L} \parallel (Z_2 + R_F)} \quad (3)$$

$$Z_2 = Z_{2\_S} \parallel Z_{2\_L} = \frac{Z_{2\_S} \cdot Z_{2\_L}}{Z_{2\_S} + Z_{2\_L}} \quad (4)$$

I_{1_L} and I_{1_F} are expressed as a function of I_{1_CT} and are given in (5) and (6).

$$I_{1\_L} = \frac{Z_2 + R_F}{Z_{1\_L} + Z_2 + R_F} \cdot I_{1\_CT} \quad (5)$$

$$I_{1\_F} = \frac{Z_{1\_L}}{Z_{1\_L} + Z_2 + R_F} \cdot I_{1\_CT} \quad (6)$$

I_{2_F} has the same magnitude, but opposite sign compared to I_{1_F}, so relation (7) is valid during the PP fault.

$$I_{2\_F} = -\frac{Z_{1\_L}}{Z_{1\_L} + Z_2 + R_F} \cdot I_{1\_CT} \quad (7)$$

Furthermore, I_{2_L} and I_{2_CT} are calculated as a function of I_{1_F} and are given in (8) and (9).

$$I_{2\_L} = \frac{Z_{2\_S}}{Z_{2\_S} + Z_{2\_L}} \cdot I_{1\_F} \quad (8)$$

$$I_{2\_CT} = \frac{Z_{2\_L}}{Z_{2\_S} + Z_{2\_L}} \cdot I_{1\_F} \quad (9)$$

The zero-sequence impedances are not involved in the PP fault, so the zero-sequence components of the current are 0 in

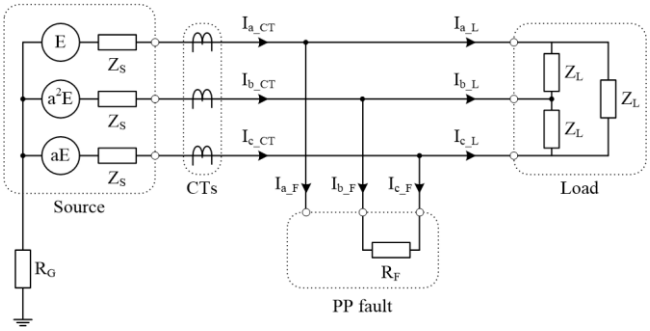

Fig. 1: Simplified electric network in PP fault conditions

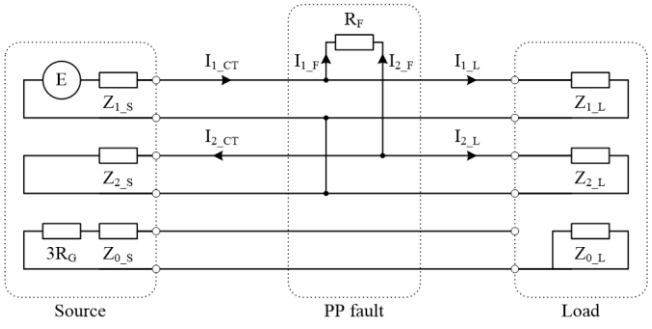

Fig. 2: Equivalent sequence diagram of the simplified electric network

this situation, as shown by (10).

$$I_{0\_CT} = I_{0\_F} = I_{0\_L} = 0 \tag{10}$$

Only I_{1_CT} and I_{2_CT} are available for protection purposes in the considered network, as only these quantities are accessible to the indicated CTs. Therefore, detection of the PP fault relies only on I_{1_CT} and I_{2_CT}, as presented in the next section.

C. Detection of the Phase-Phase fault

I_{2_CT} is 0 in healthy conditions, as the considered network is balanced and is different from 0 during the PP fault, as shown by (9). However, instead of using directly the value of I_{2_CT} to detect the PP fault, this paper proposes utilisation of the ratio between I_{2_CT} and I_{1_CT} as a fault indicator. Both I_{2_CT} and I_{1_CT} are proportional to the available short-circuit power, but their ratio varies less than I_{2_CT} with the change of the short-circuit power of the network, which is convenient for protection.

The ratio between I_{2_CT} and I_{1_CT} is a complex quantity and is expressed in relation (11), where the minus sign is due to the fact that I_{1_CT} and I_{2_CT} flow in opposite directions at the location of the CTs in the analysed circuit. Indeed, I_{1_CT} flows out of the source, while I_{2_CT} flows into the source, as indicated in Fig. 2, thus their opposite direction of flow is detected by the indicated CTs.

$$\frac{I_{2\_CT}}{I_{1\_CT}} = -\frac{Z_{2\_L}}{Z_{2\_S} + Z_{2\_L}} \cdot \frac{Z_{1\_L}}{Z_{1\_L} + Z_2 + R_F} \tag{11}$$

I_{2_CT}/I_{1_CT} ratio can be calculated by a digital relay from the CT current using relation (1) and its magnitude is always 0 in healthy conditions for a balanced network. Even in a slightly unbalanced electric network, the magnitude of I_{2_CT}/I_{1_CT} ratio is close to 0, as $I_{1\_CT} >> I_{2\_CT}$ in such conditions. During the PP fault, the magnitude of the I_{2_CT}/I_{1_CT} ratio is higher than 0, but it does not exceed 1, as revealed by examination of (11). The maximum magnitude of I_{2_CT}/I_{1_CT} ratio is reached if the PP fault occurs in no load conditions ($Z_{1\_L} = Z_{2\_L} = \infty$), while its argument is 180° in this case.

The ratio of negative over positive-sequence components is defined in (12) for the load current and even though it is not accessible to the indicated CTs, it represents the ratio seen by a hypothetic relay placed downstream the fault.

$$\frac{I_{2\_L}}{I_{1\_L}} = \frac{Z_{2\_S}}{Z_{2\_S} + Z_{2\_L}} \cdot \frac{Z_{1\_L}}{Z_2 + R_F} \tag{12}$$

Similarly to the I_{2_CT}/I_{1_CT} ratio, the I_{2_L}/I_{1_L} ratio is an indicator of the PP fault, as its magnitude is always 0 in healthy conditions for a balanced network and different from 0 during the fault. However, the maximum magnitude of the I_{2_L}/I_{1_L} ratio is not limited to 1, but it depends on sequence impedances of the network. Moreover, both I_{1_L} and I_{2_L} flow into the load, as indicated in Fig. 2, so the argument of the I_{2_L}/I_{1_L} ratio differs significantly from the argument of the I_{2_CT}/I_{1_CT} ratio for the same parameters of the circuit. This idea is illustrated in TABLE I, where both ratios are evaluated for different network conditions, assuming that the fault resistance is much smaller than the load impedance.

TABLE I. I_{2_CT}/I_{1_CT} AND I_{2_L}/I_{1_L} RATIOS FOR DIFFERENT CONDITIONS

Ratio	Magnitude	Argument	Conditions
$\frac{I_{2\_CT}}{I_{1\_CT}}$	≈ 1	$\approx 180°$	$Z_{1\_L} >> Z_{1\_S}$ $Z_{2\_L} >> Z_{2\_S}$ $Z_{1\_L} >> R_F$
$\frac{I_{2\_L}}{I_{1\_L}}$	$\approx \frac{Z_{1\_L}}{Z_{2\_L}}$	$\approx \angle Z_{1\_L} - \angle Z_{2\_L}$	
$\frac{I_{2\_CT}}{I_{1\_CT}}$	≈ 1	$\approx 180°$	$Z_{1\_L} >> Z_{1\_S}$ $Z_{2\_L} >> Z_{2\_S}$ $Z_{1\_L} >> R_F$ $Z_{1\_L} = Z_{2\_L}$
$\frac{I_{2\_L}}{I_{1\_L}}$	≈ 1	$\approx 0°$	
$\frac{I_{2\_CT}}{I_{1\_CT}}$	$\neq 0$	$\approx 180°$	$Z_{1\_L} \approx Z_{1\_S}$ $Z_{2\_L} \approx Z_{2\_S}$ $Z_{1\_L} >> R_F$
$\frac{I_{2\_L}}{I_{1\_L}}$	$\neq 0$	$\approx 0°$	
$\frac{I_{2\_CT}}{I_{1\_CT}}$	0	not defined	$R_F = \infty$ (no fault)
$\frac{I_{2\_L}}{I_{1\_L}}$	0	not defined	

The conditions assumed in TABLE I are convenient from a mathematical perspective because they allow estimation with ease of the magnitude and argument of the proposed ratios. Yet these conditions could also make sense from a technical point of view. For example, the positive-sequence impedance and the negative-sequence impedance of a non-rotating consumer are equal. The equivalent impedance of the source is much smaller than the load impedance, if the rated power of the latter is much smaller than the rated power of the source. Such a condition is not unusual in a radial feeder where a single power source supplies several loads. Contrariwise, the equivalent impedances of the source and of the load are not too different if their rated powers are similar.

TABLE I indicates that a PP fault produce different ratios of negative-sequence over positive-sequence components for the CT current and load current in the assumed conditions of the network. More precisely, a relay placed downstream the fault sees the I_{2_L}/I_{1_L} ratio, while a relay placed upstream the fault sees the I_{2_CT}/I_{1_CT} ratio. The magnitude of these ratios cannot be used to discriminate the fault direction, but only as an indicator of the fault presence in the network. However, the arguments of I_{2_L}/I_{1_L} and I_{2_CT}/I_{1_CT} ratios differs significantly during the fault, thus representing a clear indicator of the fault direction. This behaviour is convenient for a relay using the ratio of negative to positive-sequence current for protection of a radial feeder, as it can be used to detect location of the fault.

III. PROTECTION OF A RADIAL FEEDER

A. I_{2_CT}/I_{1_CT} ratio in a radial feeder

Further examination of the I_{2_CT}/I_{1_CT} ratio suggest that in a radial feeder, the closest upstream relay to the PP fault notices

the highest magnitude of the I_{2_CT}/I_{1_CT} ratio. This principle is demonstrated using a simple radial feeder whose equivalent diagram of sequence impedances is illustrated in Fig. 3.

The radial feeder consists from a power source and 2 loads and is monitored by 2 sets of CTs, named *CT1* and *CT2*, but which are not represented in Fig. 3. Z_{1_S}, Z_{2_S} and Z_{0_S} represent the positive, negative and zero-sequence impedances of the source, while Z_{1_L1}, Z_{1_L2}, Z_{2_L1}, Z_{2_L2} and Z_{0_L1}, Z_{0_L2} are the positive, negative, respectively zero-sequence impedances of the loads. I_{1_L1}, I_{1_L2}, I_{2_L1}, I_{2_L2} and I_{0_L1}, I_{0_L2} are the positive, negative, respectively zero-sequence components of the load currents, while I_{1_CT1}, I_{1_CT2}, I_{2_CT1}, I_{2_CT2} and I_{0_CT1}, I_{0_CT2} are the positive, negative, respectively zero-sequence components of the currents monitored by the considered CTs.

A PP fault is applied between *Load 1* and *Load 2* in such way that both *CT1* and *CT2* will be located upstream the applied fault. In this case, the relations (13) and (14) can be determined from Fig. 3.

$$\mathrm{I}_{1\_CT1} = \mathrm{I}_{1\_CT2} + \mathrm{I}_{1\_L1} \tag{13}$$

$$\mathrm{I}_{2\_CT1} = \mathrm{I}_{2\_CT2} - \mathrm{I}_{2\_L1} \tag{14}$$

From equations (13) and (14), relation (15) is obtained and further on relation (16) is determined, thus demonstrating that in a radial feeder the closest upstream relay to the PP fault depicts the highest magnitude of the I_{2_CT}/I_{1_CT} ratio.

$$\frac{\mathrm{I}_{2\_CT1}}{\mathrm{I}_{1\_CT1}} = \frac{\mathrm{I}_{2\_CT2} - \mathrm{I}_{2\_L1}}{\mathrm{I}_{1\_CT2} + \mathrm{I}_{1\_L1}} \tag{15}$$

$$\left|\frac{\mathrm{I}_{2\_CT1}}{\mathrm{I}_{1\_CT1}}\right| < \left|\frac{\mathrm{I}_{2\_CT2}}{\mathrm{I}_{1\_CT2}}\right| \tag{16}$$

Based on (16) and using communication it is possible to coordinate the upstream relays in such way that only the relay closest to the fault location will trip. Such coordination is not feasible in the absence of a load placed between 2 consecutive relays, as the magnitude of their ratios will be equal in this case. For example, if *Load 1* is disconnected from the grid, then I_{2_CT1}/I_{1_CT1} and I_{2_CT2}/I_{1_CT2} are equal and (16) is no longer valid in this case. However, coordination is not critical in this situation, as it makes no difference if an electric fault is cleared by the relay associated with *CT1* or by the relay associated with *CT2*, as long as *Load 2* is offline.

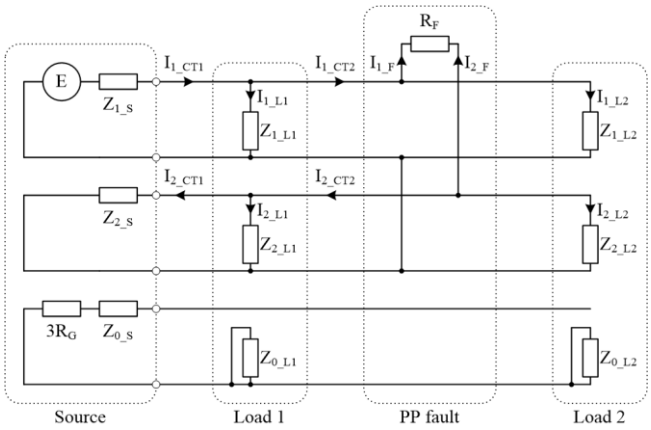

Fig. 3: Equivalent sequence diagram of a simple radial feeder

B. *Transformer's effect on I_{2_CT}/I_{1_CT} ratio*

Propagation of the current sequence components in a radial feeder is affected by the presence of a power transformer on their path. For example, the zero-sequence current cannot pass through a delta-wye transformer [7]. Moreover, the delta-wye transformer introduces a phase shift in the positive-sequence and negative-sequence currents flowing through it because of the relative phase shift between the primary and the secondary windings [7]. Therefore, the ratio of negative-sequence and positive-sequence components of the primary, respectively secondary currents is also shifted in the case of a delta-wye transformer. This holds for a wye-delta transformer as well.

The calculation procedure of the phase shifts introduced by a transformer to the symmetrical components of its voltage and current is presented in [7]. The same procedure is applied in this paper to calculate the phase shifts introduced by various transformers to the negative and positive-sequence currents and further on to calculate the phase shifts associated with the ratio of negative and positive-sequence current. The results are given in TABLE II, where the following notations are used: I_{1_p}, I_{2_p} and I_{1_s}, I_{2_s} are the positive, respectively negative-sequence currents of the primary, respectively secondary windings and n is the turns-ratio of the transformer. The phase shift of the ratio of negative to positive-sequence current is independent on whether the wye winding represents the primary or secondary side of the transformer. However, the phase shift depends on the vector group of the transformer, as shown in TABLE II.

For the investigated vector groups, the ratio of negative to positive-sequence current is shifted ±60°. Therefore, the relays placed on both sides of a transformer will notice a 60° phase difference of their I_{2_CT}/I_{1_CT} ratio. The PP fault produces about 180° phase difference between the I_{2_CT}/I_{1_CT} ratios seen by the upstream, respectively downstream relay, as shown in previous sections. If the PP fault occurs at the terminals of the power transformer, then the effect of the fault overlaps with the effect of the transformer on the I_{2_CT}/I_{1_CT} ratio. Such condition gives a phase difference between the I_{2_CT}/I_{1_CT} ratios seen by the upstream, respectively downstream relays of about ±120°, rather than 180°. Consequently, the phase shift caused by a

TABLE II. PHASE SHIFTS INTRODUCED BY A POWER TRANSFORMER TO THE SECONDARY SIDE QUANTITIES IN TERMS OF PRIMARY SIDE QUANTITIES

Vector group	Current-sequence components		$\frac{\mathrm{I}_{2\_s}}{\mathrm{I}_{1\_s}}$ ratio
	I_{1_s}	I_{2_s}	
YNd1	$n\sqrt{3}\mathrm{I}_{1\_p}\angle+30°$	$n\sqrt{3}\mathrm{I}_{2\_p}\angle-30°$	$\frac{\mathrm{I}_{2\_p}}{\mathrm{I}_{1\_p}}\angle-60°$
YNd11	$n\sqrt{3}\mathrm{I}_{1\_p}\angle-30°$	$n\sqrt{3}\mathrm{I}_{2\_p}\angle+30°$	$\frac{\mathrm{I}_{2\_p}}{\mathrm{I}_{1\_p}}\angle+60°$
Dyn1	$\frac{n}{\sqrt{3}}\mathrm{I}_{1\_p}\angle+30°$	$\frac{n}{\sqrt{3}}\mathrm{I}_{2\_p}\angle-30°$	$\frac{\mathrm{I}_{2\_p}}{\mathrm{I}_{1\_p}}\angle-60°$
Dyn11	$\frac{n}{\sqrt{3}}\mathrm{I}_{1\_p}\angle-30°$	$\frac{n}{\sqrt{3}}\mathrm{I}_{2\_p}\angle+30°$	$\frac{\mathrm{I}_{2\_p}}{\mathrm{I}_{1\_p}}\angle+60°$

power transformer on the ratio of negative to positive-sequence current should be compensated in a radial feeder.

IV. Description of the Test Maritime Feeder

The proposed protection method is investigated using the test MV feeder presented in Fig. 4. The test feeder is part of a larger maritime MV network and it can be powered by 2 diesel generators labelled G_1 and G_2. It consists of 5 loads placed on 5 bus bars that are interconnected through several cables. Also, a power transformer *Tr.* exists between *Bus 2* and *Bus 3*, while a Circuit Breaker (CB) is placed at the both ends of each cable in order to isolate a possible electric fault. The electric cables are denoted L_{xy}, where *x* and *y* are the indicators of the adjacent bus bars. The CBs are not illustrated in Fig. 4 in order to avoid over-congestion of the diagram.

The test feeder is implemented in PSCAD. The standard models available in PSCAD for a three-phase transformer, respectively combustion engine and synchronous machine are used for modelling of the power transformer, respectively diesel generators. The main parameters of these equipment are given in TABLE III for generator and in TABLE IV for the transformer. The electric cables are modelled using a π-model based on the parameters given in TABLE V. The electric loads

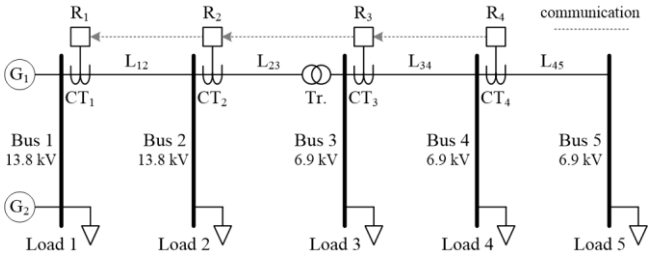

Fig. 4: Test MV radial feeder

are unbalanced consumers, with the exception of *Load 1* and are modelled as constant power loads. The power factor of the loads is set to *0.88* and their main data is given in TABLE VI.

The test feeder is protected by 4 relays placed at the feeding end of each cable and denoted R_x, where *x* is the indicator of the feeding bus bar. Each relay monitors the feeder current at its own location using a set of CTs, denoted CT_x and computes the I_{2_CT}/I_{1_CT} ratio, denoted I_{2_CTx}/I_{1_CTx}, where *x* is the indicator the relay. A communication channel is set in such way that a relay can access the I_{2_CT}/I_{1_CT} ratio calculated by the adjacent downstream relay. Therefore, each relay has access to its own ratio, respectively to the ratio provided by the adjacent relay

TABLE III. Diesel Generator Data

Parameters	G_1	G_2
Synchronous machine		
Rated power [kVA]	7200	4800
Rated voltage [kV]	13.8	13.8
Rated frequency [Hz]	50.0	50.0
Stator resistance [p.u.]	0.01	0.015
Stator reactance [p.u.]	0.11	0.08
d-axis synchronous reactance [p.u.]	1.8	1.65
d-axis transient reactance [p.u.]	0.275	0.225
d-axis subtransient reactance [p.u.]	0.185	0.145
q-axis synchronous reactance [p.u.]	1.15	1.15
q-axis subtransient reactance [p.u.]	0.205	0.195
d-axis transient time [s]	0.550	0.42
d-axis subtransient time [s]	0.08	0.06
q-axis subtransient time [s]	0.08	0.06
Inertia constant [s]	2.0	1.5
Grounding resistance [kΩ]	0.4	0.4
AC exciter type	AC1A	AC1A
Internal combustion engine		
Rated output power [kW]	6000	4000
Rated speed [rpm]	1500	1500
Gearbox ratio	1	1
Gearbox efficiency	0.98	0.98
Regulator type	PI	PI
Regulator proportional gain	12.5	12.5
Regulator integral time constant [s]	0.075	0.075
Regulator output upper limit	1.2	1.2
Regulator output lower limit	0	0

TABLE IV. Transformer Data

Parameters	Tr.
Rated power [kVA]	2000
Primary voltage [kV]	13.8
Secondary voltage [kV]	6.9
Copper losses [p.u.]	0.009
Iron losses [p.u.]	0.002
Short-circuit impedance [p.u.]	0.090
No-load current [%]	1
Vector group	Dyn11
Grounding resistance [kΩ]	0.2

TABLE V. Electric Cables Data

Cable	Resistance [mΩ]	Inductance [μH]	Capacitance/2 [nF]
L_{12}	52.4	37.6	29.3
L_{23}	10.48	7.52	5.86
L_{34}	26.8	33.1	37.1
L_{45}	14.54	7.94	5.22

TABLE VI. Consumer Data

Load name	Consumed power [kVA]		
	Phase a	Phase b	Phase c
Load 1	600	600	600
Load 2	500	450	450
Load 3	200	225	225
Load 4	150	175	175
Load 5	100	100	125

and based on these information only, the relay closest to the fault location should trip. The I_{2_CTx}/I_{1_CTx} ratios are examined in order to evaluate the feasibility of the proposed protection method in the test maritime feeder.

V. Simulation Results

A. Fault levels for the bolted Phase-Phase fault

A PP fault is applied alternatively at the end of the primary zone of protection of each relay between *phase b* and *phase c* for various network conditions. In other words, the PP fault is applied on each bus bar from *Bus 2* to *Bus 5*. The short-circuit current seen by each relay for a bolted fault occurring on its primary zone of protection is given in TABLE VI on 13.8 kV base for various network conditions. It is clear that the conventional OC protection would have been affected by the variable fault currents of the test feeder and this issue would have been even more pronounced for a resistive fault. The reduced impedance between two consecutive relays represent another issue for the OC relays, as the fault currents noticed by R_3 and R_4, for example, are practically the same.

B. I_{2_CT}/I_{1_CT} ratio seen by the relays

Considering the protection method proposed in this paper, for each of the applied faults, each relay notices an I_{2_CT}/I_{1_CT} ratio. As these ratios are complex quantities, they are plotted in the complex plane for 10 periods of time (200 ms) after the fault inception, with a time step of 1 ms. Fig. 5a illustrates the I_{2_CT}/I_{1_CT} ratio of each relay for a PP fault on *Bus 2* with a fault resistance of 2 Ω, while the test MV network is powered by G_1 only. Such fault resistance is typical for an arcing fault occurring in a MV power system similar to the considered test maritime feeder [8]. As it can be seen in Fig. 5a, the I_{2_CT}/I_{1_CT} ratio of each relay merges in a confined area of the complex plane. The mean value of the ratios seen by each relay is included in the figure.

According to Fig. 5a, the PP fault is detected by all relays, as indicated by the non-zero magnitude of the I_{2_CT}/I_{1_CT} ratios, but only R_1 trips, as the difference between the argument of R_1 (170°) and the argument of R_2 (17.4°) is significant (152.6°), so they indicate different directions for the fault. The ratios seen by R_3 and R_4 are shifted by 60° by *Tr.* and compensation of this phase shift will place them in the same zone of the complex plane as the ratio seen by R_2, therefore indicating that the PP fault occurs upstream the feeder. Indeed, after compensation the arguments of R_3 and *R4* will be 16.9°, respectively 15.7°, which again, differs significantly from the argument of the ratio seen by R_1.

TABLE VII. Fault current on 13.8 kV base seen by each relay for an PP bolted fault at the end of its primary zone of protection

Network conditions	Fault current [kA]			
	R_1	**R_2**	**R_3**	**R_4**
G_1 off, G_2 on	0.72	0.46	0.41	0.39
G_1 on, G_2 off	0.91	0.53	0.47	0.46
G_1 on, G_2 on	1.45	0.66	0.59	0.57

Rated currents for each relay are: R_1 120 A, R_2 60 A, R_3 33A, R_4 13A

Fig. 5b illustrates the I_{2_CT}/I_{1_CT} ratio for each relay for a PP fault on *Bus 4*, while the rest of the network conditions remain unchanged from the previous case. Again, the fault is detected by all relays, due to the non-zero magnitude of their ratios. The ratios seen by R_3 and R_4 need to be shifted by -60° in order to compensate the effect of the transformer, an operation that will place the ratios seen by R_1, R_2 and R_3 in the same zone of the complex plane, while R_4 will be placed in a completely different area. Indeed, after compensation of the phase shift introduced by *Tr.*, the arguments of the ratios seen by relays R_3 and R_4 will be 116°, respectively -40.1°, while the arguments of the ratios seen by relays R_1 and R_2 are 104°, respectively

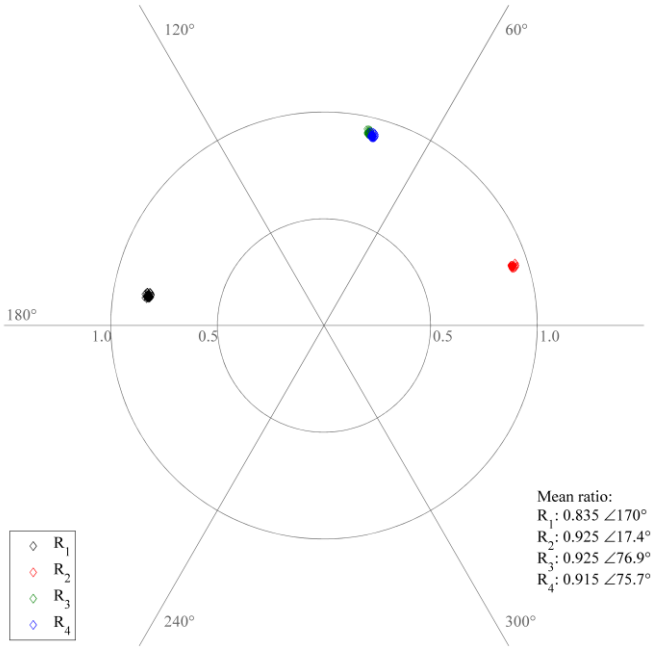

Fig. 5a: I_{2_CT}/I_{1_CT} ratio for a 2 Ω PP fault on Bus 2; G_1 on, G_2 off

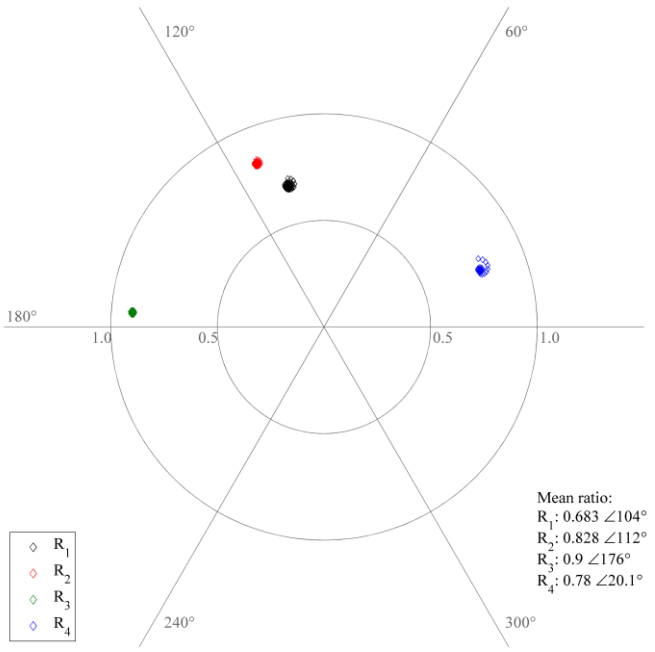

Fig. 5b: I_{2_CT}/I_{1_CT} ratio for a 2 Ω PP fault on Bus 4; G_1 on, G_2 off

112°. As a result, R_4 indicates an upstream fault, while R_1, R_2 and R_3 indicate a downstream fault. However, the fault is cleared by R_3 due to the magnitude of its ratio, which is the highest among the relays R_1, R_2 and R_3. If R_3 fails to clear the fault, then the relay with the second highest magnitude of the proposed ratio will trip, thus ensuring the backup protection.

Fig. 6a and Fig. 6b illustrate the I_{2_CT}/I_{1_CT} ratio for each relay in the case of a PP fault on *Bus 2*, respectively *Bus 4*, with a fault resistance of *2 Ω*, while the test MV network is powered by G_2 only. The same fault is applied on the same bus bars in the case of the test MV feeder powered by both G_1 and G_2 and the results are presented in Fig 7a and Fig. 7b. In all of the considered cases, the PP faults are detected and cleared correctly. According to these figures, the region occupied by the I_{2_CT}/I_{1_CT} ratios on the complex plane does not change too much with the change of the available short-circuit power in the network, so the previous discussions are still valid.

Compared to the fault currents shown in TABLE VII, the I_{2_CT}/I_{1_CT} ratios vary less with the change of the short-circuit power caused by variable generation. These results indicate that the performance of the new protection method is superior to the conventional OC protection in a maritime radial feeder.

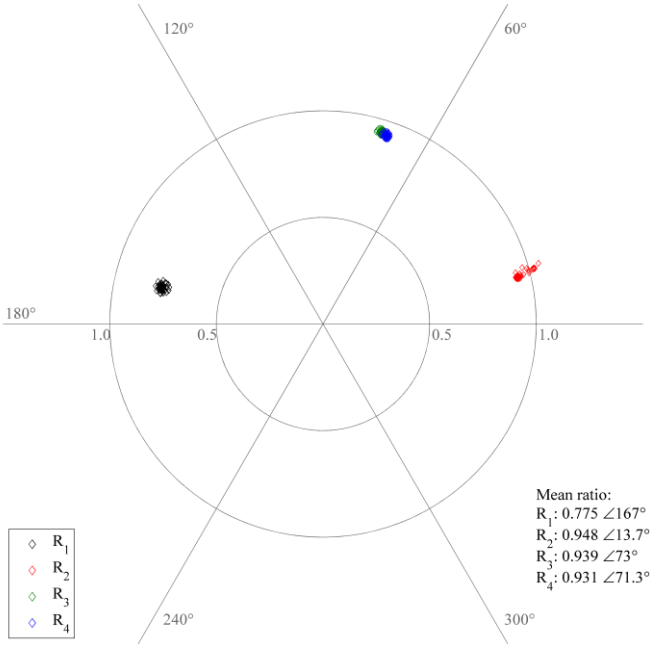

Fig. 6a: I_{2_CT}/I_{1_CT} ratio for a 2 Ω PP fault on Bus 2; G_1 off, G_2 on

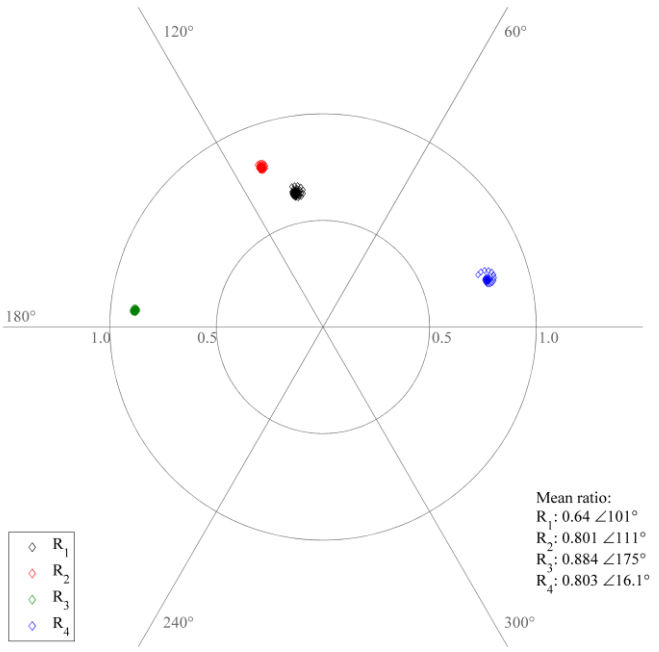

Fig. 6b: I_{2_CT}/I_{1_CT} ratio for a 2 Ω PP fault on Bus 4; G_1 off, G_2 on

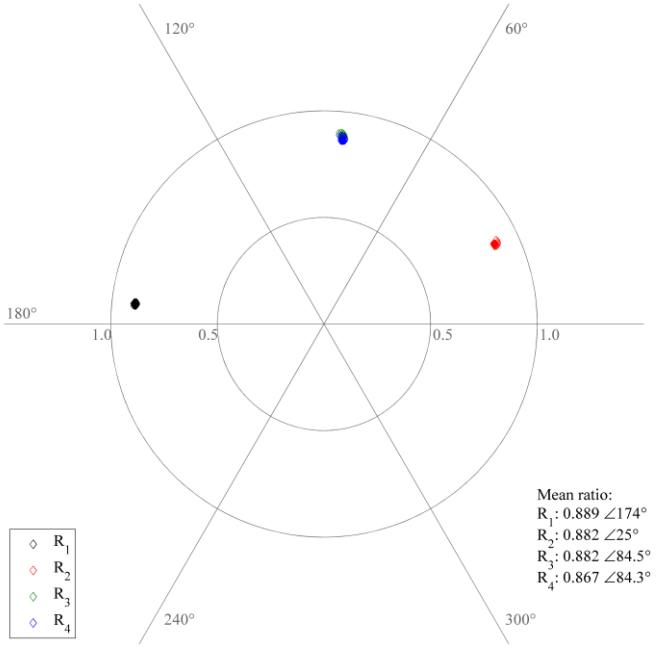

Fig. 7a: I_{2_CT}/I_{1_CT} ratio for a 2 Ω PP fault on Bus 2; G_1 on, G_2 on

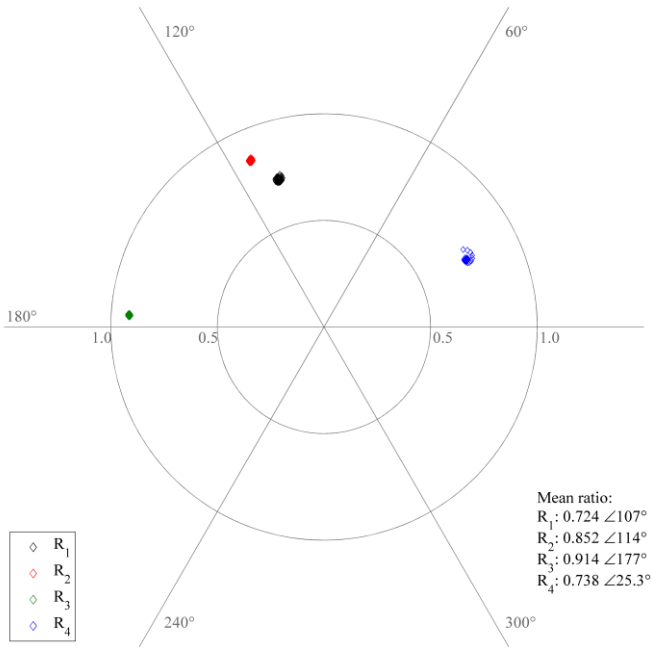

Fig. 7b: I_{2_CT}/I_{1_CT} ratio for a 2 Ω PP fault on Bus 4; G_1 on, G_2 on

VI. Conclusion

To summarize, the authors propose utilisation of the ratio of negative-sequence over positive-sequence components of the current for detection of the PP fault in a radial feeder of which level of unbalance is reasonable low. The presence of the PP fault is indicated by the magnitude of the proposed ratio, which suffers a significant increase during the fault, while the fault direction is indicated by the argument of the ratio. Moreover, the closer an upstream relay is to the PP fault, the higher the magnitude of its own ratio is and precisely this information is used to clear the PP fault in a coordinated manner.

Simulation results prove that the new protection method is feasible in a radial MV feeder and the relays are able to operate correctly even in the case of variable short-circuit power. The locus on the complex plane of the ratio of negative-sequence to positive-sequence current is dependent on fault characteristics, but has a reduced variation with the change of the short-circuit current. Moreover, the new protection method does not require prior knowledge of the fault levels in the protected feeder. The findings of this paper indicate that the proposed method of protection is superior to the OC protection in a radial feeder.

References

[1] C. I. Ciontea, C. Leth Bak, F. Blaabjerg, K. K. Madsen, C. H. Sterregaard, "Review of network topologies and protection principles in marine and offshore applications", *25th Australasian Universities Power Engineering Conference*, Wollongong, Australia, Sep. 2015

[2] K. Van Dokkum, "Ship knowledge: ship design, construction and operation", DOKMAR Maritime Publishers BV, 2013, 8th edition

[3] R. Borstlap, H. Ten Katen, "Ships' electrical systems", DOKMAR Maritime Publishers BV, 2011, 1st edition

[4] C. I. Ciontea, C. Leth Bak, F. Blaabjerg, K. K. Madsen, C. H. Sterregaard, "Decentralized adaptive overcurrent protection for medium voltage maritime power systems", *IEEE PES Asia-Pacific Power and Energy Engineering Conference*, Xi'an, China, Oct. 2016

[5] C. I. Ciontea, C. Leth Bak, F. Blaabjerg, K. K. Madsen, C. H. Sterregaard, "Fault Analysis for protection purposes in maritime applications", *IET Developments in Power System Protection Conference*, Edinburgh, UK, Mar. 2016

[6] J. L. Blackburn, "Protective Relaying: Principles and Applications", Marcel Decker, Inc., New York, USA, 1987

[7] W. A. Elmore, "Protective Relaying: Theory and Applications", Marcel Dekker, Inc., New York, USA, 2004, 2nd edition

[8] G. Ziegler, "Numerical distance protection", Publicis Publishing, Erlangen, Germany, 2011